Near-field polarimetric characterization of polymer crystallites

Lori S. Goldner,[a),b)] Scott N. Goldie,[a),c)] Michael J. Fasolka,[d)] Francoise Renaldo,[a)] Jeeseong Hwang,[a)] and Jack F. Douglas[d)]
National Institute of Standards and Technology, Gaithersburg, Maryland 20899

(Received 16 January 2004; accepted 15 June 2004)

We use near-field polarimetry (NFP) to investigate thin-film crystallites of isotactic polystyrene (iPS). NFP micrographs enable quantitative optical characterization of the birefringence in these specimens with subdiffraction-limited resolution, resulting in observations that give: (1) evidence for radial strain in the depletion boundary surrounding the growth front, and (2) a map of local tilt in the crystal axis and/or strain in the amorphous layers above and below the growth plane of the crystallites. [DOI: 10.1063/1.1785866]

Polymer crystallization has been studied for many decades, yet significant questions persist regarding both the morphology of polymer crystallites and the mechanisms by which they form. Particularly in "cold" crystallization of ultrathin films ($<$100 nm), where crystallites form quasi-two dimensionally out of an amorphous matrix, crystallite morphologies exist that are not seen in the bulk, and confinement raises challenging questions regarding how random polymer coils transform into ordered crystals.[1] A full understanding of these systems is confounded by the difficulty of studying thin films. Traditional scattering, optical, and microscopy techniques elucidate some aspects of crystallite morphology and fine structure in thin systems. However, such methods often lack spatial resolution and/or sensitivity required to examine: (1) chain conformations near the growth front, (2) amorphous layers posited to exist over and under these thin crystals, and (3) the orientation of folded chains within these crystallites. Here, we use near-field polarimetry (NFP) to measure the retardance and fast axis orientation of crystallites in isotactic polystyrene (iPS) thin films, and thereby elucidate structure and the character of the strain field in these nonequilibrium patterns with a lateral resolution of about 50 nm.

Polymers crystallize by forming folded layers (lamellae). In iPS, these lamellae organize on a larger scale into hexagonal crystals with a sixfold symmetry around the chain (c) axis; polystyrene is a uniaxial crystal with a fast c axis. In a sufficiently thin film (thickness $<$ the radius of gyration of the polymer, R_g), crystallites one lamella thick form into various hexagonally symmetric or irregular branching morphologies. A boundary depleted of polymer (depletion boundary) forms as polymer from the amorphous region is pulled into the crystallite region.[2] Taguchi *et al.*[3,4] suggest that, for films one lamella thick, even crystallites with a disordered appearance (seaweed) are actually single crystals with the c axis perpendicular to the substrate except for a small tilt ($<6°$) perpendicular to the local growth direction. At the top and bottom surfaces of the crystallite, polymer chains loop back on themselves and a thin amorphous layer is expected and has been reported.[2] In thicker films, the lamellae stack and the chain axis can tilt or twist.[5] An amorphous layer above the folded lamellae and a depletion region around the growing crystal pattern should still be present.

Polarimetry enables measurement of the retardance and fast axis orientation. Traditional polarimetric techniques have lateral resolution limited to a few millimeters, while micropolarimeters have micron resolution. To better elucidate the structure in early growth-stage crystallites, we apply polarization-modulation polarimetry using a near-field scanning optical microscope (NSOM). Transmission aperture NSOM achieves superresolution by illuminating a thin specimen with light confined to a subwavelength aperture.[6] By positioning the sample in the near field of the aperture, the confined light transmits through the sample to be collected via conventional optics. Micrographs, acquired by scanning the sample and measuring the transmitted intensity at each point, exhibit resolution determined by the aperture width. While scanning, the sample-to-aperture distance is maintained to $\leqslant$10 nm using a shear-force feedback system,[7] which also yields the sample topography. With NFP, images of retardance and fast axis orientation in thin films can be obtained with lateral resolution between 50 nm and 150 nm. Details of instrumentation and analysis can be found in Refs. 8 and 9.

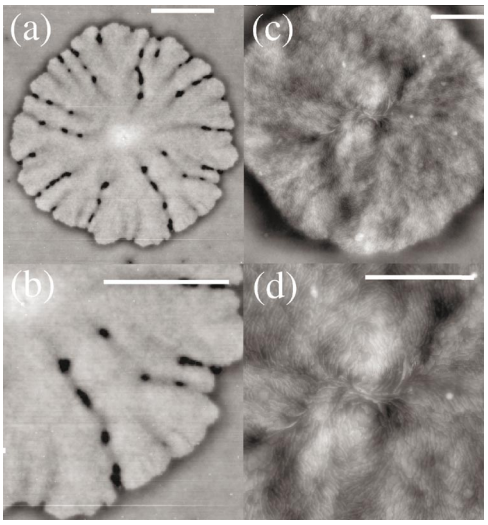

FIG. 1. (Color) Topographic AFM of crystallites. Dendrite (a,b) with detail of bottom right corner (0 nm–51 nm). Spherulite (c,d) with detail of central region (0 nm–25 nm). Scale bars are 1 μm.

[a)]Optical Technology Division, Physics Laboratory, Stop 8443.
[b)]Electronic mail: lori.goldner@nist.gov
[c)]Current address: Shire Laboratories, Rockville, MD 20850.
[d)]Polymers Division, Materials Science and Engineering Laboratory, Stop 8542.

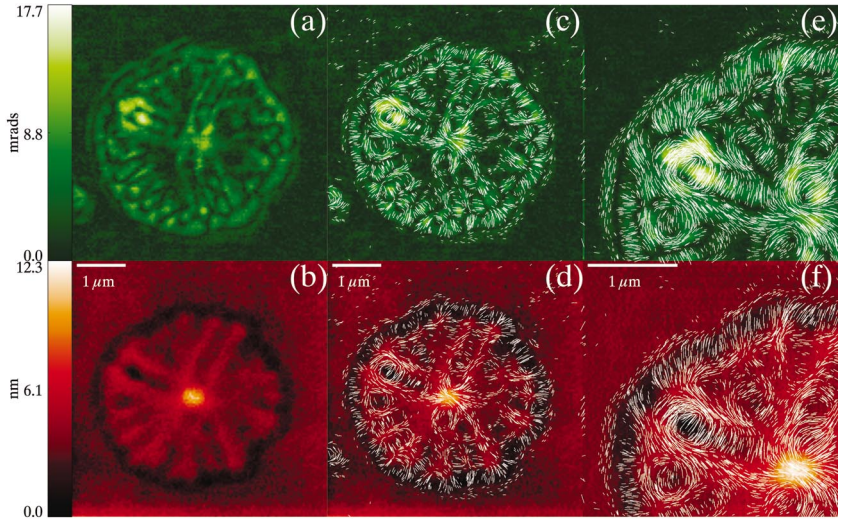

FIG. 2. (Color) Retardance and topography images of seaweed crystallites. (a), retardance; (b), topography; (c), retardance with overlaid fast axis orientation; (d), topography with overlaid fast axis orientation; (e,f), higher resolution scan of upper left quadrant.

For a uniaxial crystal, the optical retardance through a film of thickness t with a fast (c) axis tilted out of the plane is given by $\theta = 2\pi \cdot (n_o - n') \cdot t/\lambda$, where the effective index of refraction n' is given by $1/n' = \sqrt{\cos^2\alpha/n_o^2 + \sin^2\alpha/n_e^2}$.[10] Here, α is the angle of the c axis with respect to the normal to the substrate, λ is the wavelength of light, and n_e and n_o are the extraordinary (here along the fast or chain axis) and ordinary indices of refraction. For iPS, we take the birefringence of the crystalline form to be $n_o - n_e = 0.28$.[11,12] An amorphous polymer material under stress also exhibits birefringence with a corresponding retardance, $\theta = 2\pi \cdot \Delta n \cdot t \cdot f/\lambda$.[13] Here, f is an orientation factor that is 1 for perfectly aligned chains, and $\Delta n = 0.167$[11,14,15] is the intrinsic birefringence of the polymer. For polystyrene, the average index $n = 1.6$.[15] For the c axis perpendicular to the substrate, $\alpha = 0$ and the crystalline fraction contributes zero retardance. Strain in the amorphous layer and depletion boundary contributes a retardance depending on the magnitude of f.

NFP images of retardance and fast axis orientation are obtained following Ref. 8. In these measurements, the effect of sample diattenuation and NSOM probe and background diattenuation and retardance have been removed,[8] resulting in a measurement of sample retardance alone. Fast axis orientation is measured with respect to an unknown axis, and so in the data below an overall angular shift has been applied as described.

Thin films of iPS were prepared by spin-coating diluted stock solutions [90% iPS (molecular mass, $M_r = 6 \times 10^5$, and polydispersity index, $M_r/M_n = 3.0$)] in toluene (mass fraction 4.5%) purchased from Scientific Polymer Products][16] onto No. 1 glass coverslips. A 1% mass fraction solution was used for the film with spherulites; film thickness was 85 nm ± 4 nm measured with an ultraviolet–visible reflectance interferometer. Samples were dried under a vacuum for 72 h. Heating on a 160 °C hotplate for 2 h (followed by quenching) resulted in spherulite crystals with an approximate radius of 1.5 μm in an amorphous matrix, as verified by optical and atomic force microscopy (AFM).

Dendritic patterns with seaweed morphology[17] were grown in a thinner film, spin cast from a 0.5 mass fraction iPS/toluene solution. The film thickness, ≈15 nm, was measured as above. To improve the adhesion of the ultrathin film to the glass, the substrates were cleaned in piranha solution (70/30 H_2SO_4/H_2O_2) rinsed in deionized H_2O, and then dried under anhydrous N_2. Clean substrates were then subjected to n-octyldimethylchlorosilane vapor for 60 min, rinsed with toluene, and baked 2 h at 125 °C, resulting in a hydrophobic monolayer. Cast iPS films were dried under vacuum for 72 h. Crystallization was induced through baking on a 160 °C hotplate for 1 h, after which the films were quenched to room temperature to arrest further growth. Dendritic "seaweed"[17] crystallites in an amorphous matrix were verified via AFM.

In Fig. 1 we show AFM images of crystallites in the same films studied by NFP in Figs. 2 and 3. For the dendrites, the thickness of the films is less than the R_g of the iPS (22 nm), so crystallites are a single lamella thick. In the multilamellar spherulites, individual lamellae are visible in Fig. 1(d) and a characteristic sheaflike structure is visible at the center. In all cases, a depletion region, with low topography, is seen around the edges, and a thick nucleation site is visible in the center.

NFP images of a seaweed dendrite are shown in Fig. 2. The topography images are of a lower resolution than those of Fig. 1; good NSOM tips are flat across the bottom with a diameter ≈400 nm,[6] resulting in poor topographic images. Figure 2(a) clearly shows a birefringent structure growing in an amorphous ($\theta = 0$) background. Areas of high birefringence are seen at the center of the pattern (nucleation site), around the edges (in the depletion boundary, 6 mrad $< \theta <$ 10 mrad) and near the growth tips. A very small θ is also visible in a ring outside the depletion layer; it is possible that this small θ is an artifact of tip/sample coupling. The fast (c) axis orientation is shown with lines overlaid on the retardance and topography images in Figs. 2(c) and 2(d). A second scan of the top left quadrant, taken at higher resolution, is shown in Figs. 2(e) and 2(f). The fast axis lines are drawn with the length proportional to the local θ; no lines are drawn for $\theta < 2.7$ mrad. An overall angular shift of 0.50 rad has been applied to all fast axis data to bring polymer in the depletion region into radial alignment. The noise floor (precision) is 1 mrad (standard deviation).

If the c axis of the crystal deviates from normal by $< 6°$,[3,4] then a 15 nm thick crystal should have $\theta < 1$ mrad.

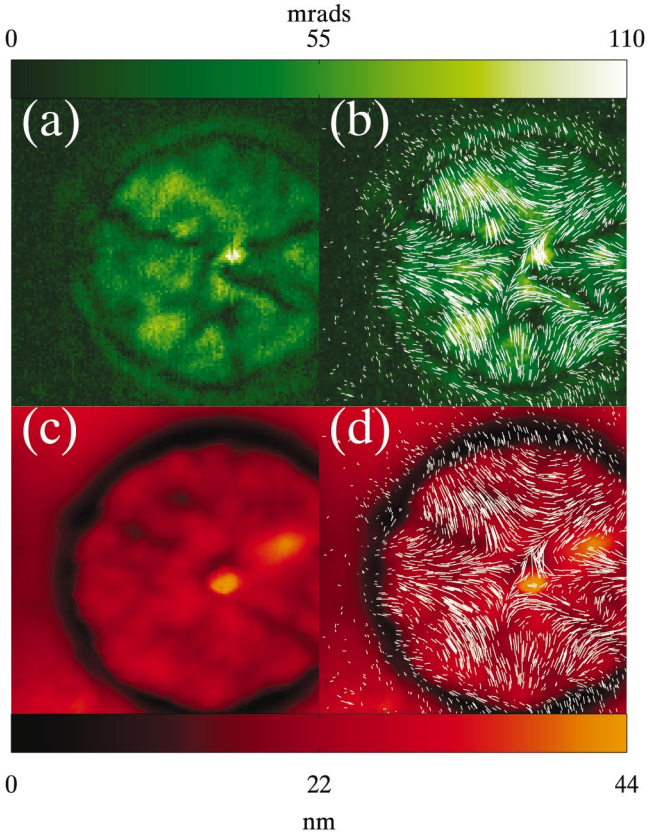

FIG. 3. (Color) Retardance (a, b) and topography (c,d) images of spherulitic crystallite, with overlaid fast axis orientation in (b) and (d).

The observed retardance therefore cannot be the result of chain tilt in the lamellae alone. However, a stressed amorphous layer only 5 nm thick could have $\theta = 10$ mrad for $f = 1$. The central nucleation site in Fig. 2 has a clear unidirectional strain, the largest evident in this image, with a sheaflike appearance to the strain that is reminiscent of an early growth morphology of spherulites.[18] A secondary nucleation site appears to be visible in the top left corner. For a 15 nm thick film, the maximum retardance ($f = 1$) is 32 mrad, and so stress in amorphous regions or layers can account for most of the retardance observed in Fig. 2.

In Fig. 3, we show NFP images of a spherulite. The topographic image is shifted slightly to the left of the optical image, an artifact of the geometric details of the NSOM tip. Spherulites are multilayered and the chain axis will tilt in the circumferential direction.[5] Around the growth boundary, we again see a depletion region consistent with radial strain ($20 \text{ mrad} < \theta < 30 \text{ mrad}$) if a 0.8 rad angular shift is applied to the fast axis data. Healing of the fast axis direction from radial to circumferential as we move in radially toward the center of the spherulite is evident, except for six angles at which the radial alignment persists to the center. Similar behavior was seen in a second isolated spherulite; a spherulite that bordered another spherulite along one side was similar except only five radial incursions were seen. Here, the noise floor is 4 mrad.

For iPS, the maximum retardance for 84 nm thick films is 211 mrad ($f = 1$), roughly twice the measured maximum. The retardance measured in Fig. 3 is greater than could possibly be due to strain in thin amorphous layers, but less than is possible for crystalline iPS perfectly aligned with *c* axis parallel to the substrate. It seems likely that these images reflect a combination of contributions arising from strain in the amorphous regions and tilt of the chain axis.

For both dendritic and spherultic crystallites in these ultrathin films, subsequent scans with different NSOM tips gave NFP images that were quantitatively similar to those shown in Figs. 2 and 3. For crystals where the *c* axis is perpendicular to the substrate, the retardance from crystal birefringence is zero and we directly image the orientation of the amorphous layer. If the thickness of the amorphous layer can be determined, this would permit a direct measurement of stresses on the polymer that may affect its morphology and crystallite growth dynamics.[4]

One of the authors (S.N.G.) is grateful to the National Research Council for a National Institute of Standards and Technology Postdoctoral Research Fellowship. Funding for this work was through the NIST Advanced Technology Program and Physics Laboratory. The authors also thank Kathryn Beers of the Polymers Division, NIST, for assistance in preparing the film specimens.

[1] K. Izumi, P. Gan, M. Hashimoto, A. Toda, H. Miyaji, Y. Miyamoto, and Y. Nakagawa, in *Advances in the Understanding of Crystal Growth Mechanisms*, edited by T. Nishinaga, K. Nishioka, J. Harada, A. Sasaki, and H. Takei, Elsevier, Amsterdam, 1997), p. 337; R. L. Jones, S. K. Kumar, D. L. Ho, R. M. Briber, and T. P. Russell, Macromolecules **34**, 559 (2001); O. Mellbring, S. K. Oiseth, A. Krozer, J. Lausmaa, and T. Hjertberg, *ibid.* **34**, 7496 (2001); G. Reiter, Europhys. Lett. **23**, 579 (1993); G. Reiter and J.-U. Sommer, J. Chem. Phys. **112**, 4376 (2000); Y. Sakai, M. Imai, K. Kaji, and M. Tsuji, J. Cryst. Growth **203**, 244 (1999); S. Sawamura, H. Miyaji, K. Izumi, S. I. Sutton, and Y. Miyamoto, J. Phys. Soc. Jpn. **67**, 3338 (1998).
[2] K. Izumi, P. Gan, A. Toda, H. Miyaji, M. Hashimoto, Y. Miyamoto, and Y. Nakagawa, Jpn. J. Appl. Phys., Part 2 **33**, L1628 (1994).
[3] K. Taguchi, H. Miyaji, K. Izumi, A. Hoshino, Y. Miyamoto, and R. Kokawa, Polymer **42**, 7443 (2001); K. Taguchi, H. Miyaji, K. Izumi, A. Hoshino, Y. Miyamoto, and R. Kokawa, J. Macromol. Sci., Phys. **41**, 1033 (2002).
[4] K. Taguchi, Y. Miyamoto, H. Miyaji, and K. Izumi, Macromolecules **36**, 5208 (2003).
[5] B. Wunderlich, *Macromolecular Physics* (Academic, New York, 1973).
[6] E. Betzig, J. K. Trautman, T. D. Harris, J. S. Weiner, and R. L. Kostelak, Science **251**, 1468 (1991).
[7] E. Betzig, P. L. Finn, and J. S. Weiner, Appl. Phys. Lett. **60**, 2484 (1992).
[8] L. S. Goldner, M. J. Fasolka, S. Nougier, H. P. Nguyen, G. W. Bryant, J. Hwang, K. D. Weston, K. L. Beers, A. Urbas, and E. L. Thomas, Appl. Opt. **42**, 3864 (2003).
[9] M. J. Fasolka, L. S. Goldner, J. Hwang, A. M. Urbas, P. DeRege, T. Swager, and E. L. Thomas, Phys. Rev. Lett. **90**, 016107 (2003).
[10] G. F. Harding, in *Optical Properties of Polymers*, edited by G. H. Meeten (Elsevier, London, 1986), p. 63.
[11] E. F. Gurnee, J. Appl. Phys. **25**, 1232 (1954).
[12] R. S. Stein, J. Appl. Phys. **32**, 1280 (1961).
[13] Z. Tadmor and G. G. Costas, *Principles of Polymer Processing* (Wiley, New York, 1979).
[14] V. N. Tsevtkov, J. Polym. Sci. **57**, 727 (1962).
[15] J. C. Seferis, in *Polymer Handbook*, edited by J. Brandrup, E. H. Immergut, and E. A. Grulke (Wiley, New York, 1999).
[16] Certain commercial equipment, instruments, or materials are identified in this letter to foster understanding. Such identification does not imply recommendation or endorsement by the National Institute of Standards and Technology, nor does it imply that the materials or equipment identified are necessarily the best available for the purpose.
[17] E. Brener, H. Muller-Krumbhaar, and D. Tempkin, Europhys. Lett. **17**, 535 (1992); V. Ferreiro, J. F. Douglas, J. Warren, and A. Karim, Phys. Rev. E **65**, 042802 (2002); V. Ferreiro, J. F. Douglas, J. A. Warren, and A. Karim, Phys. Rev. E **65**, 051606 (2002); E. Brener, H. Muller-Krumbhaar, D. Tempkin, and T. Abel, Physica A **249**, 73 (1998).
[18] D. R. Norton and A. Keller, Polymer **26**, 704 (1985).